FINITE ELEMENT ANALYSIS OF A NASA NATIONAL TRANSONIC FACILITY WIND TUNNEL BALANCE

Michael C. Lindell
NASA Langley Research Center
Hampton, VA

S/4-35

040-172

372467

P.

SUMMARY

This paper presents the results of finite element analyses and correlation studies performed on a NASA National Transonic Facility (NTF) Wind Tunnel balance. In the past NASA has relied primarily on classical hand analyses, coupled with relatively large safety factors, for predicting maximum stresses in wind tunnel balances. Now, with the significant advancements in computer technology and sophistication of general purpose analysis codes, it is more reasonable to pursue finite element analyses of these balances. The correlation studies of the present analyses show very good agreement between the analyses and data measured with strain gages and therefore the studies give higher confidence for using finite element analyses to analyze and optimize balance designs in the future.

INTRODUCTION

Until recent years computer software and hardware limitations have hindered the detailed analysis of strain-gage balances by finite element methods. Due to the intricate design features of balances conventional h-element finite element codes were not practical because extremely fine meshes would be required to adequately capture stress gradients within the intricate geometric regions. If such models were produced the hardware required to run a solution (memory and disk space) would typically be unavailable. Even if the hardware was available to run the solution, several runs with varying mesh size would be required for each load case to gain confidence that stress gradients were reasonably captured. Such a process would be very time-consuming. The emergence of p-element finite element codes coupled with advances in computer technology has brought the detailed analysis of strain-gage balances within the reach of desktop workstations.

The balance under investigation is shown in Figure 1 as a Parametric Technology Corporation (PTC) Pro/Engineer part model. The design is an actual balance used in the NTF (balance number NTF-101A) and is also representative of the kind of intricate features found in other types of balances. The balance is fabricated from a single piece of 200 CVM maraging steel. Room temperature material properties for this steel are shown in Table 1. Some key dimensions of the balance are shown in Figure 2.
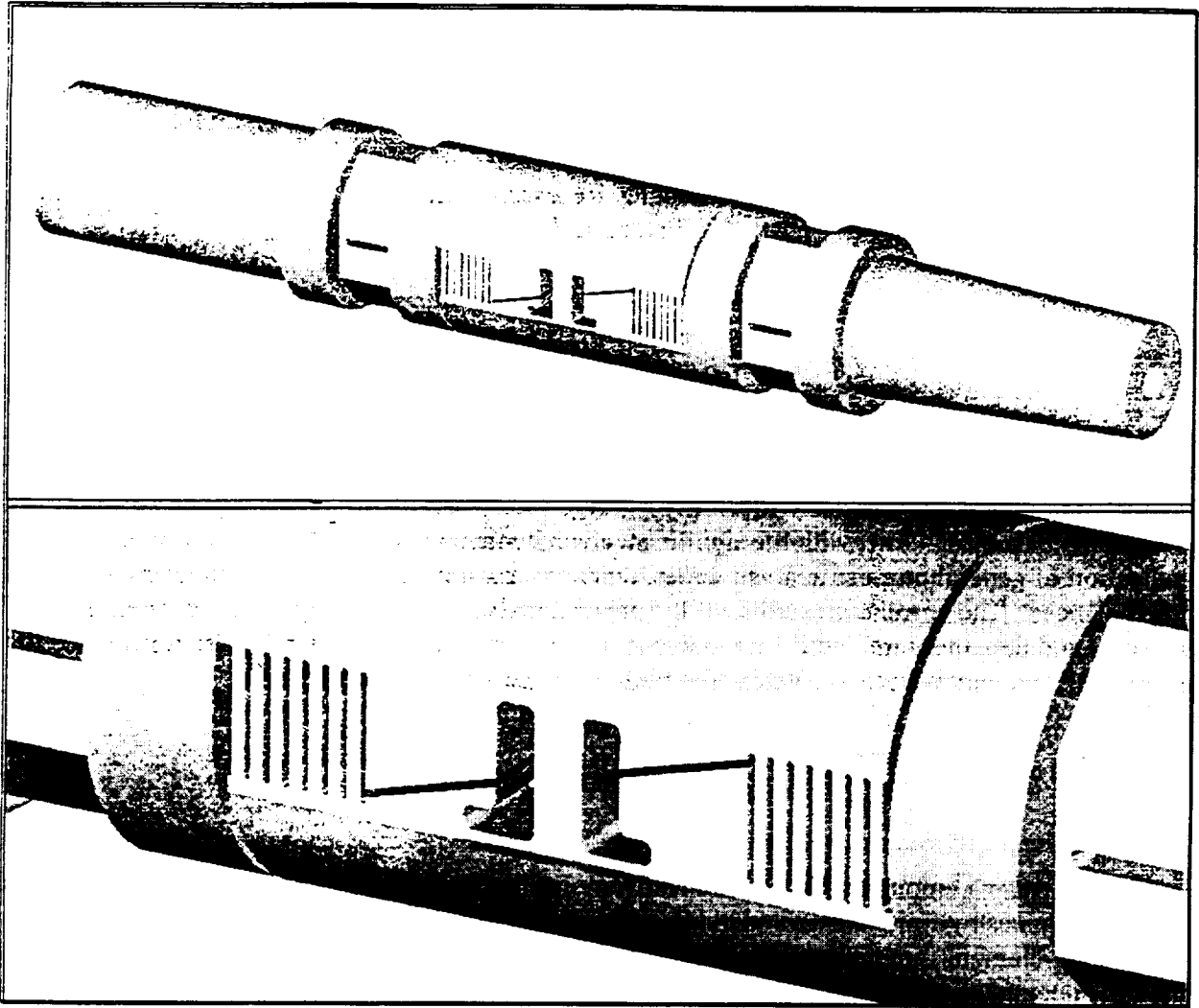
Figure 1. Pro/Engineer geometry model of NTF balance 101A.

Table 1. Room Temperature Material Properties for 200 CVM Maraging Steel

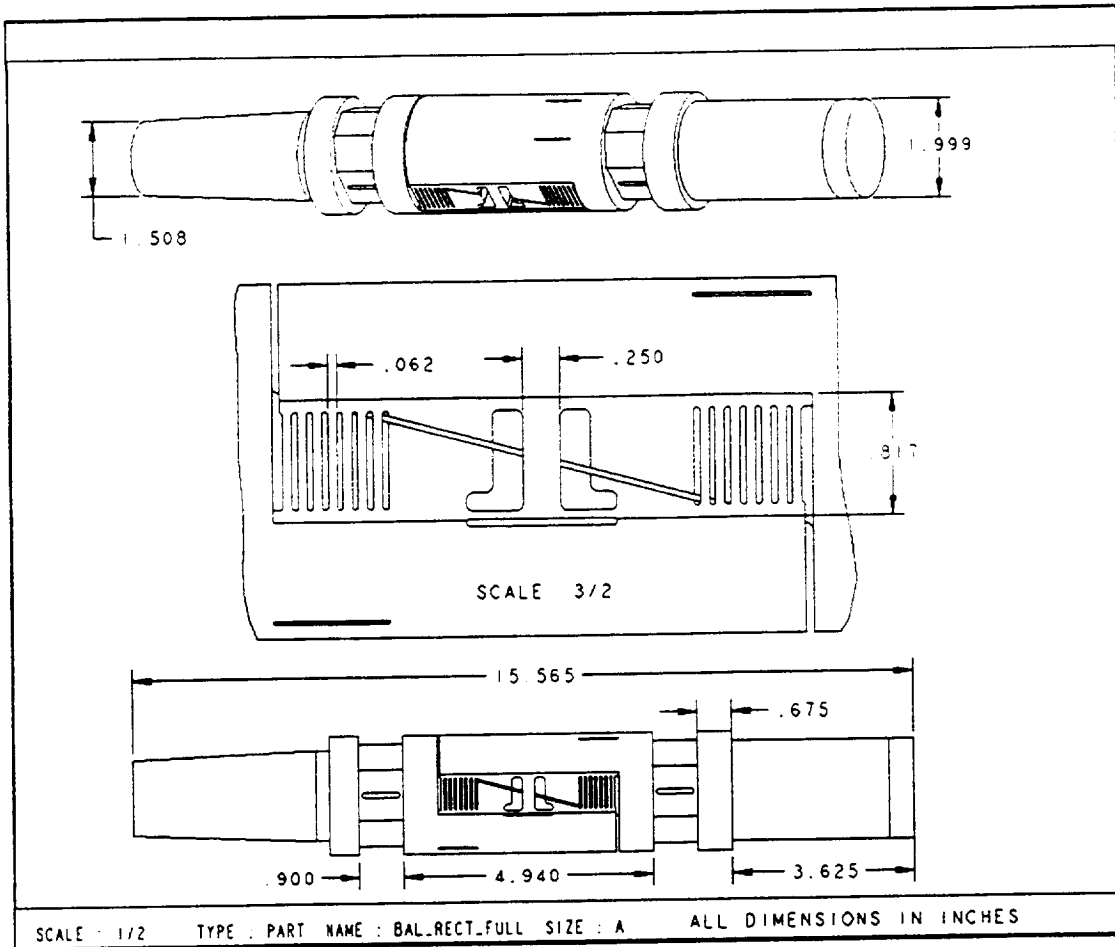| Modulus of Elasticity (psi)	26.2×10^6
Density (lb/in³)	0.289
Yield Strength (psi)	206,000
Ultimate Strength (psi)	212,000

Figure 2. General balance dimensions for NTF 101A.

ANALYSIS AND CORRELATION

The analysis code used in these analyses was PTC Pro/Mechanica, an adaptive p-element technology code. The finite element model created for the balance is shown in Figure 3. The model consists of 8,630 high-order tetrahedral solid elements. The boundary condition on the model, to reflect the test setup, has the outer surface of the tapered end completely restrained. The loads were applied, also reflecting the test setup, by distributing the loads on the surface of the non-tapered end such that the desired resultant load through the balance center was achieved. A total of seven load cases were analyzed, the first six of which were correlated with test data. The seventh load case was a combination of the first six load cases and had no test data with which to correlate. The various load cases applied to the model are shown in Table 2.
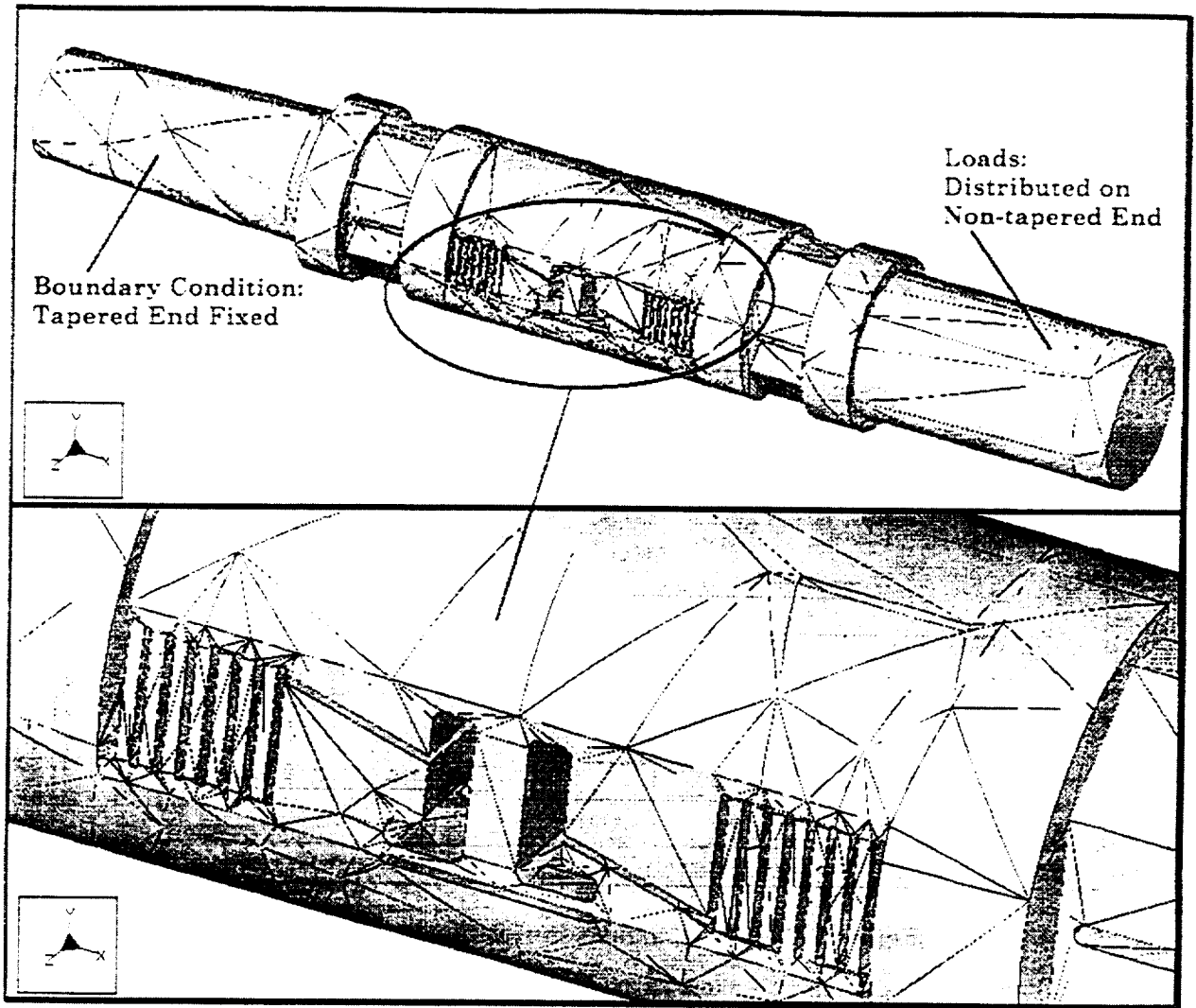
Figure 3. Mechanica model of NTF balance 101A.

Table 2. Applied Load Cases

LOAD CASE	LOAD	AXIS & DIRECTION
1. Axial Force	700 lbs	-X
2. Normal Force	5,000 lbs	-Y
3. Side Force	4,000 lbs	-Z
4. Roll Moment	8,989 in-lbs	RX
5. Yaw Moment	6,480 in-lbs	RY
6. Pitch Moment	13,000 in-lbs	-RZ
7. Combined	Above loads simultaneously	Above axes simultaneously

Load Case 1

The first load case consists of an axial force of 700 pounds applied as a compressive load on the end of the balance. Figure 4 shows a stress (σ_{YY}) fringe plot (see Report Availability section of this report for information on obtaining color versions of these plots) with exaggerated deformation for this load case. Also shown in Figure 4 is the location of the strain gage used for correlation.
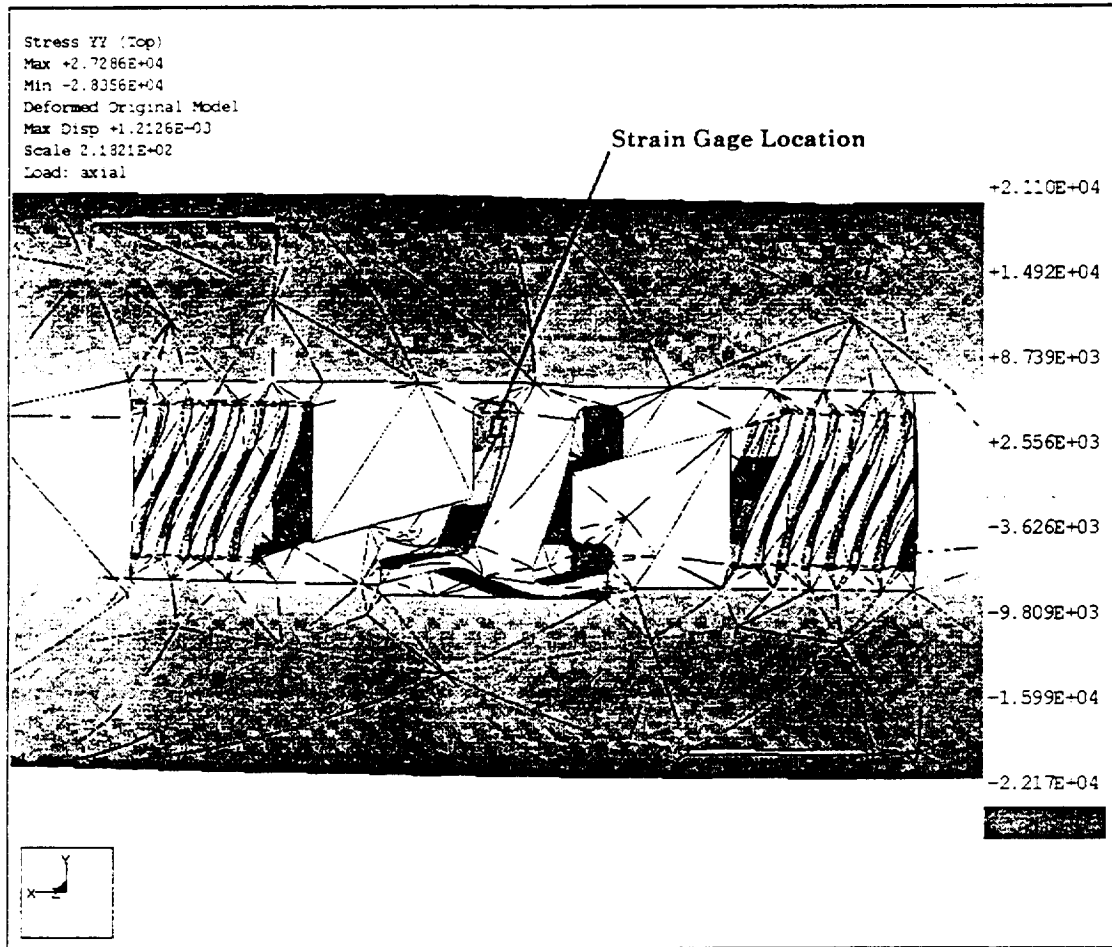

Figure 4. Axial load case stress and deformation.

The measured strain at the gage location for the axial force load condition was 499.5 microstrain ($\mu\epsilon$) (13,090 psi). The strain at the same location from the finite element analysis was 489.3 $\mu\epsilon$ (12,820 psi), a difference of -2.0%. There were no excessively high stress regions for this load case.

Load Case 2

The second load case consists of a normal force of 5,000 lbs applied in the -Y axis through the balance center. Figure 5 shows a stress (σ_{XX}) fringe plot with exaggerated deformation for this load case and shows the location of the strain gage used for correlation and also areas of relatively high stress.
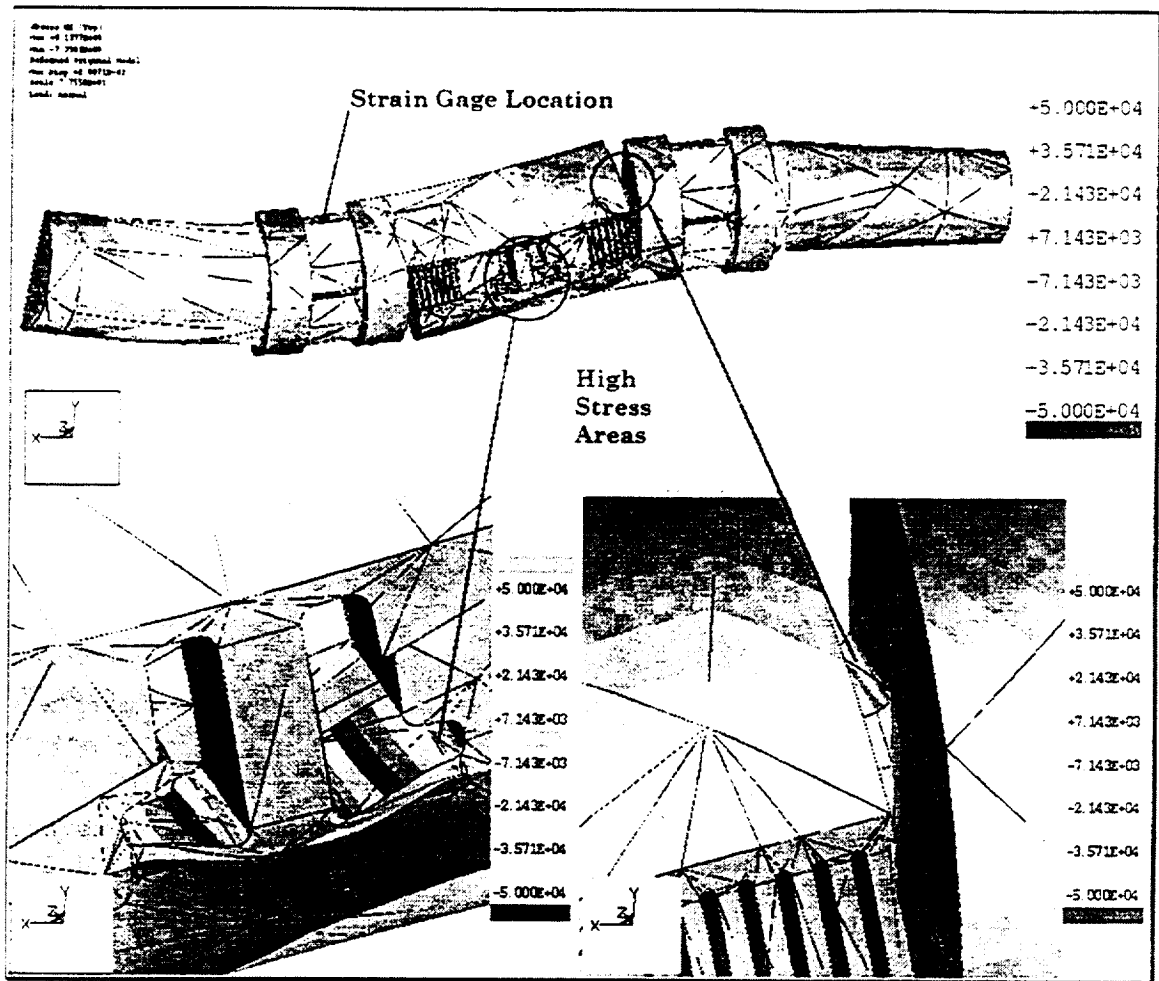
Figure 5. Normal load case stress and deformation.

The measured strain at the gage location for the normal force load condition was 720.4 $\mu\epsilon$ (18, 875 psi). The strain at the same location from the finite element analysis was 719.0 $\mu\epsilon$ (18,840 psi), a difference of -0.2%. The maximum stress (σ_{xx} stress component) in the high stress area on the right of Figure 5 was between 70,000 and 90,000 psi.

Load Case 3

The third load case consists of a side force of 4,000 lbs applied in the -Z axis through the balance center. Figure 6 shows a stress (σ_{xx}) fringe plot with exaggerated deformation for this load case. Also shown in Figure 6 is the location of the strain gage used for correlation.

The measured strain at the gage location for the side load condition was 767.0 $\mu\epsilon$ (20,095 psi). The strain at the same location from the finite element analysis was 774.1 $\mu\epsilon$ (20,280 psi), a difference of 0.9%. There were no excessively high stress areas for this load case.
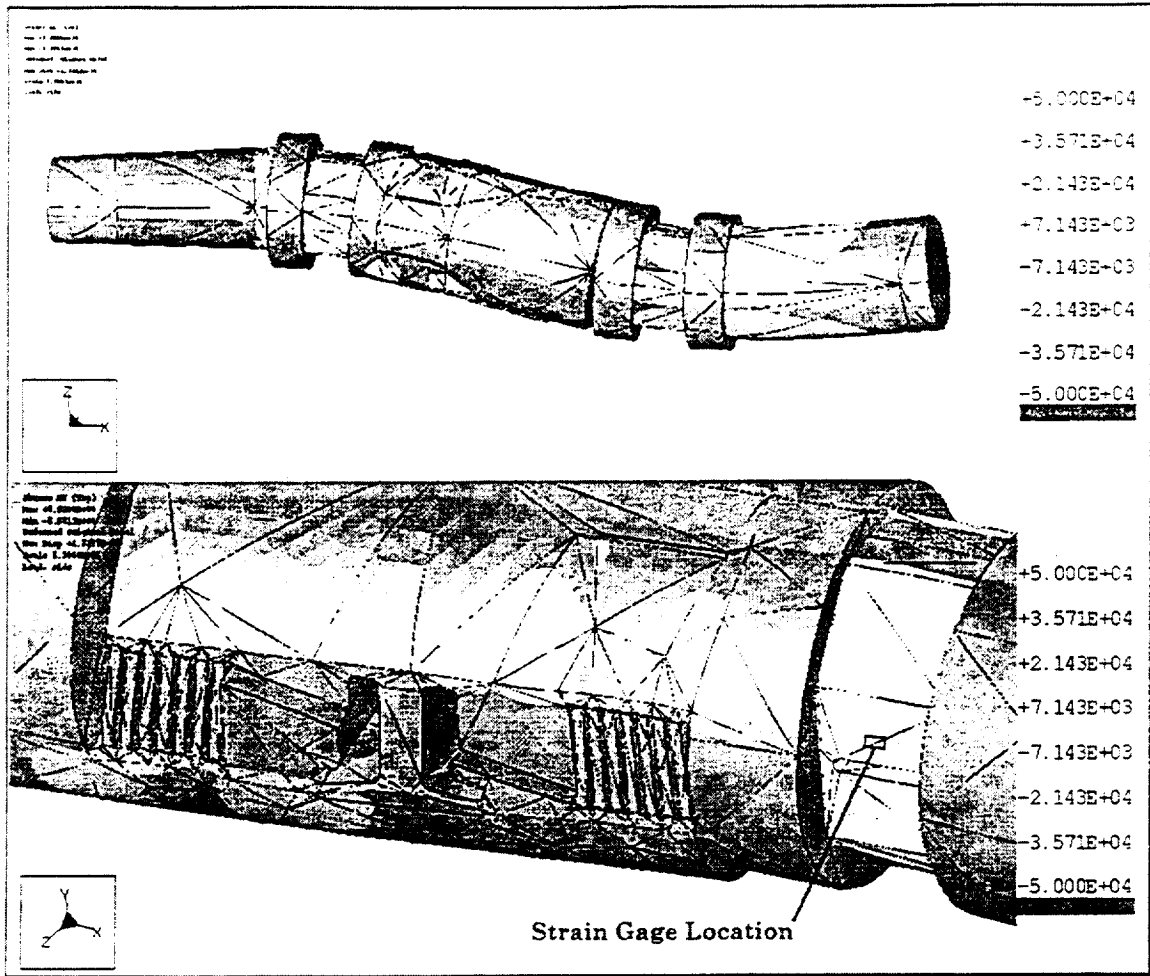
Figure 6. Side load case stress and deformation.

Load Case 4

The fourth load case consists of a roll moment of 8,989 in-lbs applied about the X axis through the balance center. Figure 7 shows a stress (σ_{xx}) fringe plot with exaggerated deformation for this load case and shows the location of the strain gage used for correlation. Also shown in Figure 7 is an area of relatively high stress.

The measured strain at the gage location for the roll moment load condition was 433.3 $\mu\epsilon$ (11,350 psi). The strain at the same location from the finite element analysis was 402.3 $\mu\epsilon$ (10,540 psi), a difference of -7.2%. The maximum stress (σ_{xx} stress component) in the high stress area was about -70,000 psi.

The figure contains stress contour scale labels. Upper scale:
+5.000E+04
+3.571E+04
+2.143E+04
+7.143E+03
-7.143E+03
-2.143E+04
-3.571E+04
-5.000E+04

Labels: High Stress Area, Strain Gage Location

Lower scale:
+5.000E+04
+3.571E+04
+2.143E+04
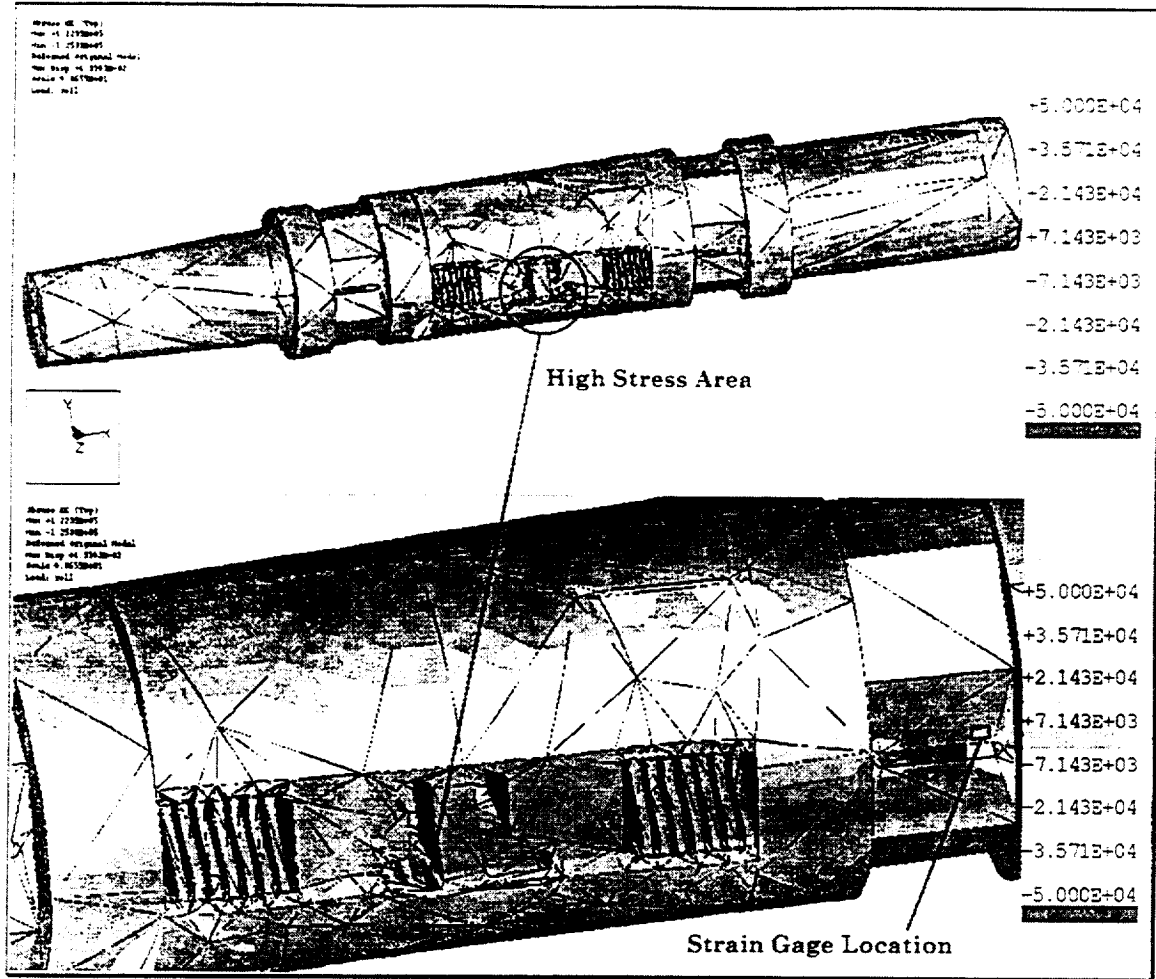+7.143E+03
-7.143E+03
-2.143E+04
-3.571E+04
-5.000E+04

Figure 7. Roll load case stress and deformation.

Load Case 5

The fifth load case consists of a yaw moment of 6,480 in-lbs applied about the Y axis through the balance center. Figure 8 shows a stress (σ_{xx}) fringe plot with exaggerated deformation for this load case. Also shown in Figure 8 are the location of the strain gage used for correlation along with an area of relatively high stress.

The measured strain at the gage location for the yaw moment load condition was 436.1 $\mu\varepsilon$ (11,425 psi). The strain at the same location from the finite element analysis was 483.1 $\mu\varepsilon$ (12,660 psi), a difference of 10.8%. The maximum stress (σ_{xx} stress component) in the high stress area was about 55,000 psi.
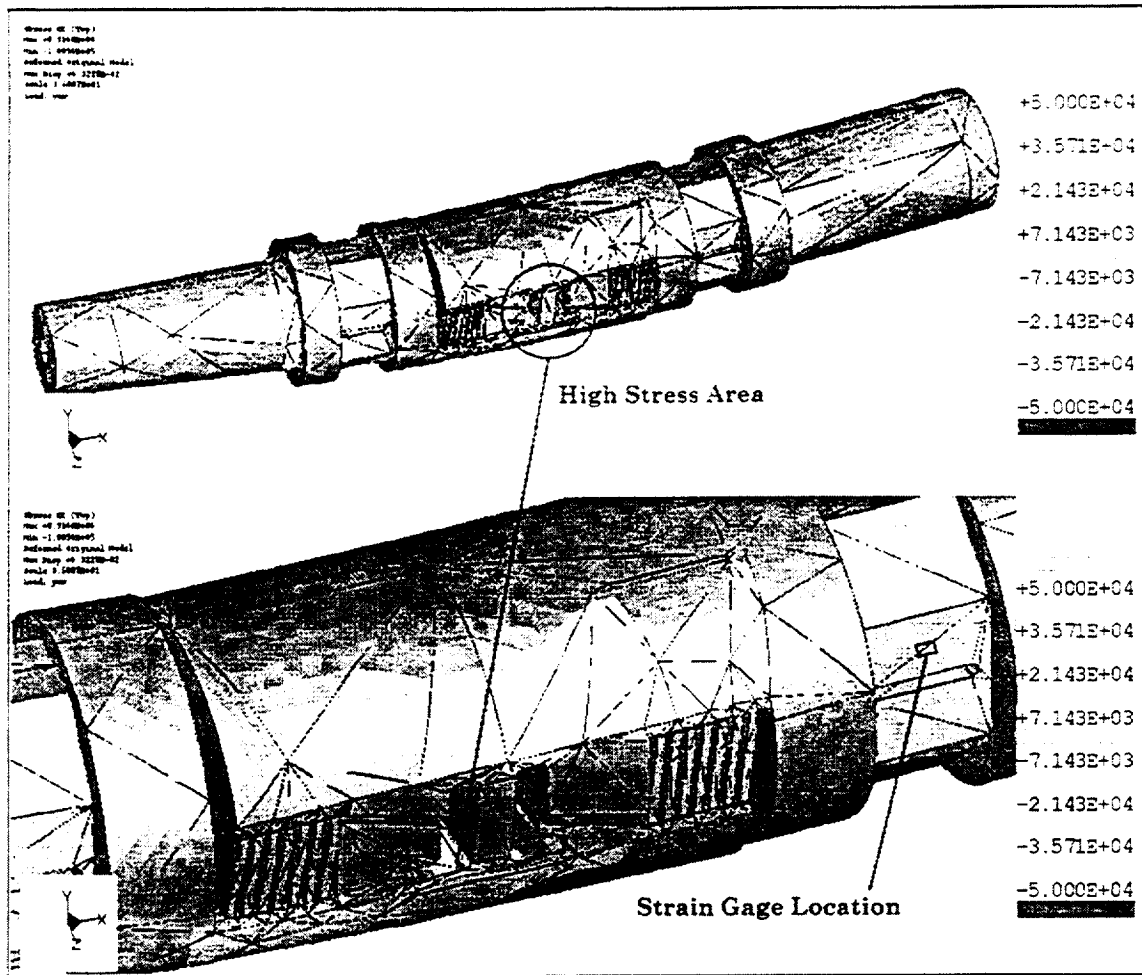
Figure 8. Yaw load case stress and deformation.

Load Case 6

The sixth load case consists of a pitch moment of 13,000 in-lbs applied about the Z axis through the balance center. Figure 9 shows a stress (σ_{xx}) fringe plot with exaggerated deformation for this load case. Also shown in Figure 9 are the location of the strain gage used for correlation along with an area of relatively high stress.

The measured strain at the gage location for the pitch moment load condition was 641.6 µε (16,810 psi). The strain at the same location from the finite element analysis was 644.7 µε (16,890 psi), a difference of 0.5%. The maximum stress (σ_{xx} stress component) in the high stress area was between 85,000 and 105,000 psi.
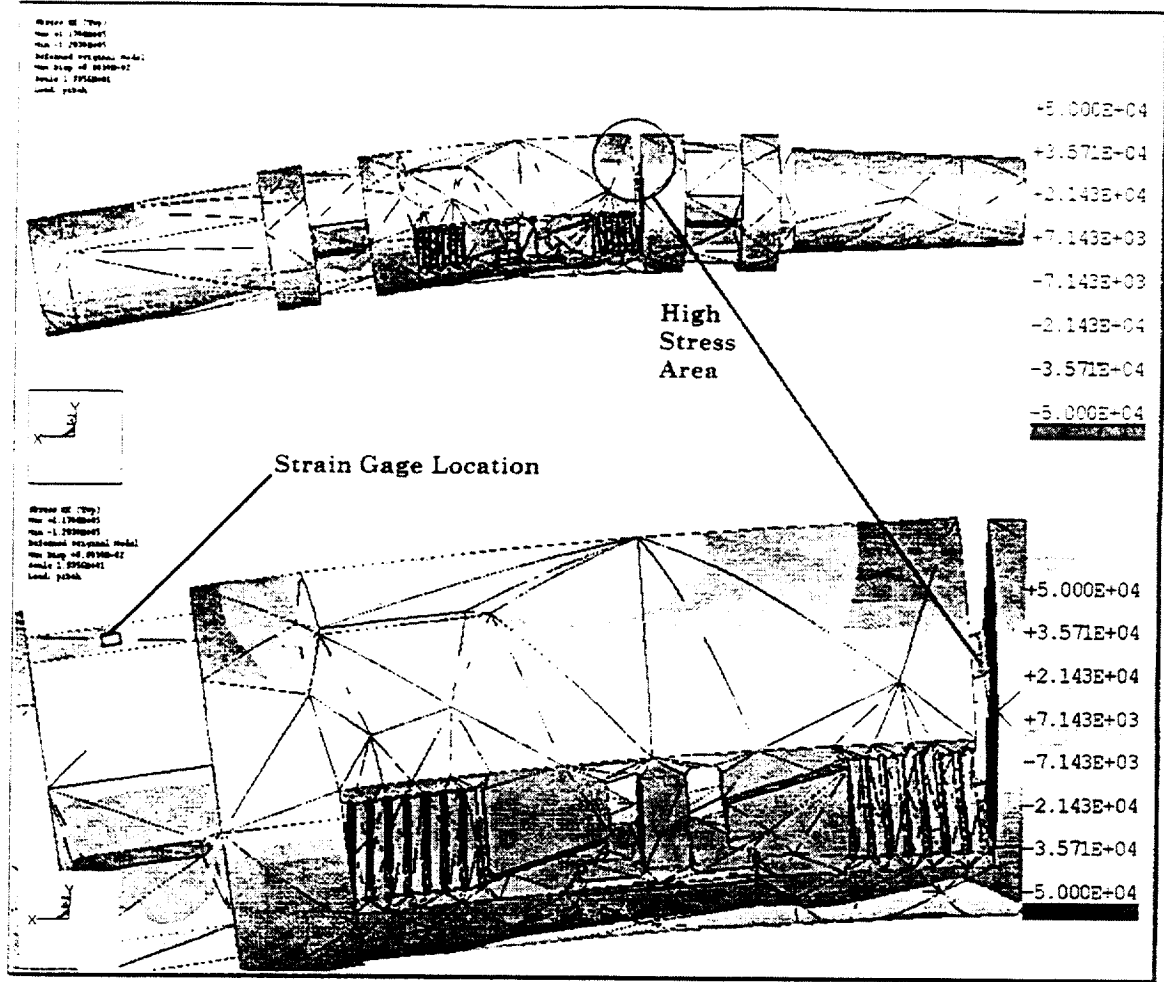
603

Figure 9. Pitch load case stress and deformation.

Load Case 7

The seventh load case is a combination of the first six load cases (-700 lbs X, -5000 lbs Y, -4000 lbs Z, 8989 in-lbs RX, 6480 in-lbs RY, -13000 in-lbs RZ). Figure 10 shows a stress (Von Mises) fringe plot with exaggerated deformation for this load case. Also shown in Figure 10 are a few areas of high stress.

The maximum stresses (Von Mises) in the high stress areas for the combined load case were in excess of 180,000 psi and approaching yield in some localized areas. A future test is planned with a strain gage in one of these high stress areas to validate this finding.
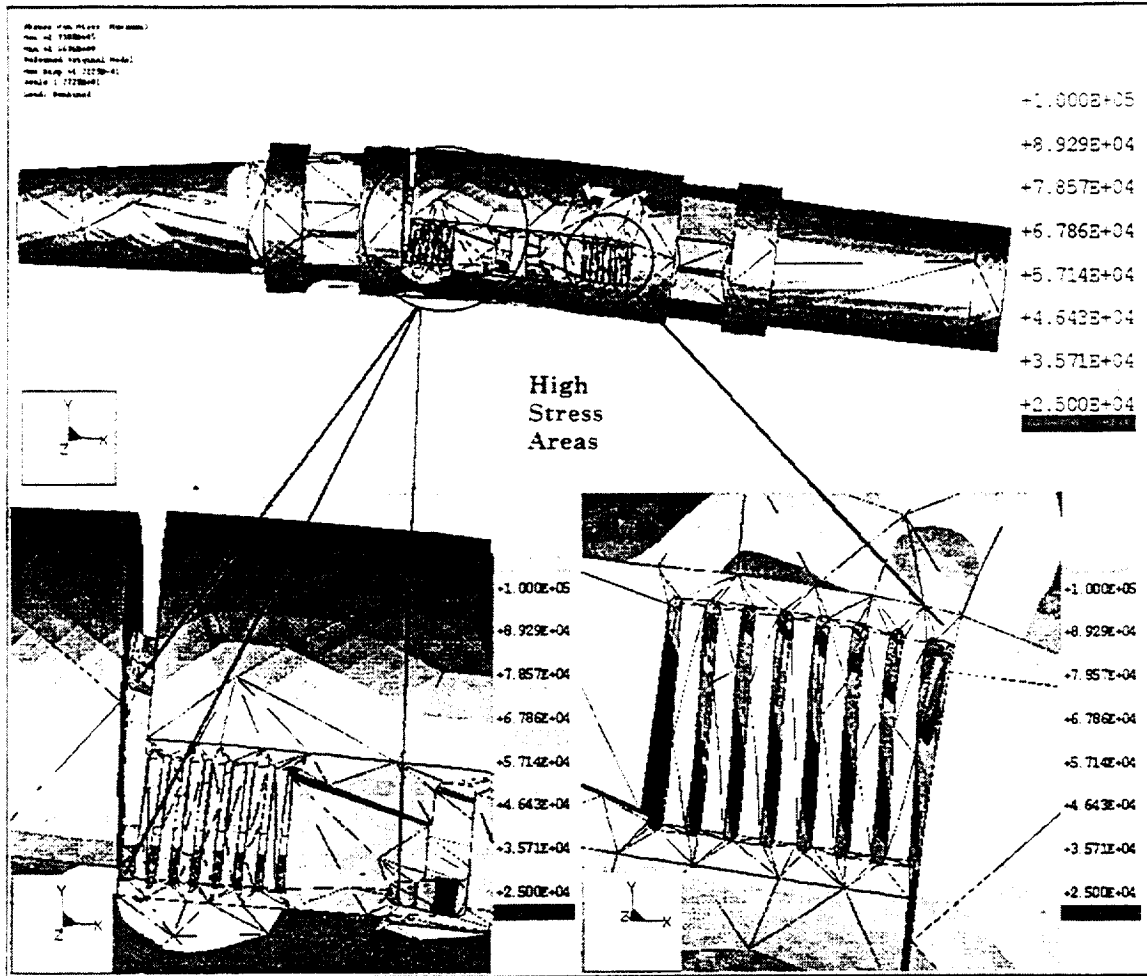
Figure 10. Combined load case stress and deformation.

Summary of Test/Analysis Correlation

Table 3 gives a summary of the degree of correlation between the measured strain and the strain computed from the finite element analyses.

Table 3. Summary of Test/Analysis Correlation

LOAD CASE	APPLIED LOAD	MEASURED STRAIN ($\mu\epsilon$)	ANALYSIS STRAIN ($\mu\epsilon$)	% DIFFERENCE
Axial Force	700 lbs	499.5	489.3	-2.0
Normal Force	5,000 lbs	720.4	719.0	-0.2
Side Force	4,000 lbs	767.0	774.1	0.9
Roll Moment	8,989 in-lbs	433.3	402.3	-7.2
Yaw Moment	6,480 in-lbs	436.1	483.1	10.8
Pitch Moment	13,000 in-lbs	641.6	644.7	0.5

CONCLUSIONS

The results of this study have shown that finite element analyses of strain-gage balances can accurately predict stress levels in the hardware. The results also showed the existence of areas within the balance where stress levels are higher than had previously been anticipated. In the future, results from such finite element analyses can be used to optimize balance designs for higher loads, reduced stress concentrations, lower weight, and reduced safety factors.

FUTURE WORK

Another balance similar to the one analyzed in this report but with more extensive strain gage instrumentation will soon be tested. An analysis and correlation study will also be performed in support of that test and the results will be documented.

ACKNOWLEDGMENTS

REPORT AVAILABILITY

This report along with full color versions of the graphics can be found on the internet at http://ixeab3.larc.nasa.gov/ntf/ntf_101a.html.